RESEARCH PAPER

Synthesis, LC-MS/MS analysis, and biological evaluation of two vaccine candidates against ticks based on the antigenic P0 peptide from *R. sanguineus* linked to the p64K carrier protein from *Neisseria meningitidis*

Luis Javier González[1] · Pedro E. Encinosa Guzmán[2] · Wendy Machado[1] · Satomy Pousa[1] · Alejandro Leyva[3,4] · Ana Laura Cano Arguelles[2] · Gleysin Cabrera[1] · Luis Ariel Espinosa[1] · Rubén Parra[1] · Rachel Hernández[1] · Yamil Bello Soto[2] · Frank L. Ledesma[2] · Marisdania Joglar[2] · Osmany Guirola[5] · Louise Ulrich Kurt[6] · Paulo C. Carvalho[6] · Ania Cabrales[7] · Hilda Garay[7] · Vladimir Besada[1] · Rosario Durán[3,4] · Toshifumi Takao[8] · Mario Pablo Estrada[2] · Alina Rodríguez-Mallon[2]

Abstract

A peptide from the P0 acidic ribosomal protein (pP0) of ticks conjugated to keyhole limpet hemocyanin from *Megathura crenulata* has shown to be effective against different tick species when used in host vaccination. Turning this peptide into a commercial anti-tick vaccine will depend on finding the appropriate, technically and economically feasible way to present it to the host immune system. Two conjugates (p64K-Cys^{1}pP0 and p64K-βAla^{1}pP0) were synthesized using the p64K carrier protein from *Neisseria meningitidis* produced in *Escherichia coli*, the same cross-linking reagent, and two analogues of pP0. The SDS-PAGE analysis of p64K-Cys^{1}pP0 showed a heterogeneous conjugate compared to p64K-βAla^{1}pP0 that was detected as a protein band at 91kDa. The pP0/p64K ratio determined by MALDI-MS for p64K-Cys^{1}pP0 ranged from 1 to 8, being 3-5 the predominant ratio, while in the case of p64K-βAla^{1}pP0 this ratio was 5-7. Cys^{1}pP0 was partially linked to 35 out of 39 Lys residues and the N-terminal end, while βAla^{1}pP0 was mostly linked to the six free cysteine residues, to the N-terminal end, and, in a lesser extent, to Lys residues. The assignment of the conjugation sites and side reactions were based on the identification of type 2 peptides. Rabbit immunizations showed the best anti-pP0 titers and the highest efficacy against *Rhipicephalus sanguineus* ticks when the p64K-Cys^{1}pP0 was used as vaccine antigen. The presence of high molecular mass aggregates observed in the SDS-PAGE analysis of p64K-Cys^{1}pP0 could be responsible for a better immune response against pP0 and consequently for its better efficacy as an anti-tick vaccine.

Keywords Anti-tick vaccine · P0 · p64K · Conjugation sites · Cross-linked peptides · Mass spectrometry

✉ Luis Javier González
luis.javier@cigb.edu.cu

✉ Alina Rodríguez-Mallon
alina.rodriguez@cigb.edu.cu

[1] Department of Proteomics, Center for Genetic Engineering and Biotechnology (CIGB), Avenida 31, e/ 158 y 190, Cubanacán, Playa, 10600 Havana, Cuba

[2] Animal Biotechnology Department, Center for Genetic Engineering and Biotechnology (CIGB), Avenida 31, e/ 158 y 190, Cubanacán, Playa, 10600 Havana, Cuba

[3] Unidad de Bioquímica y Proteómica Analítica (UByPA), Institut Pasteur de Montevideo, Mataojo 2020, Montevideo, Uruguay

[4] Instituto de Investigaciones Biológicas Clemente Estable (IIBCE), 11600 Montevideo, Uruguay

[5] Bioinformatics, Center for Genetic Engineering and Biotechnology (CIGB), Avenida 31, e/ 158 y 190, Cubanacán, Playa, 10600 Havana, Cuba

[6] Laboratory for Structural and Computational Proteomics, Carlos Chagas Institute, Fiocruz, Rua Professor Algacyr Munhoz Mader, 3775, Ciudade Industrial de Curitiba, Curitiba, Paraná 81310-020, Brazil

[7] Synthetic Peptides Laboratory, Center for Genetic Engineering and Biotechnology (CIGB), Avenida 31, e/ 158 y 190, Cubanacán, Playa, 10600 Havana, Cuba

[8] Institute for Protein Research, Osaka University, Suita Campus, Osaka 565, Japan

Introduction

Ticks are hematophagous ectoparasites that may transmit pathogens when feed on hosts, causing several deadly diseases [1]. The use of chemicals is still the main choice for controlling tick populations. However, the intensive use of these chemicals induces tick-resistant phenotypes [2, 3]. Milk and meat contamination as well as environmental pollution are also important issues for consumers. Therefore, vaccination has become an encouraging strategy to control tick infestations when included in integrated management strategies [3, 4]. Although promising antigens against ticks have been evaluated under laboratory conditions [5], only vaccines based on the concealed Bm86 antigen have been commercialized and applied under field conditions [6, 7]. The efficacy of these vaccines has been variable (51–99 %) depending on the *R. microplus* tick strain [4, 8].

Few peptides have been used as anti-tick vaccine candidates [9, 10] because they are rapidly cleared from the blood stream and are, in general, poor immunogens. Hence, peptides are generally conjugated to a highly immunogenic carrier protein to overcome this limitation.

Chemical conjugation of a 20-amino acid peptide from P0 acidic ribosomal protein of ticks (pP0) to keyhole limpet hemocyanin (KLH) from *Megathura crenulata* has shown to be effective against different tick species when used for host vaccination [9–11].

KLH as a carrier protein enabled us to advance quickly in a proof-of-concept of pP0 as a wide coverage antigen for the development of an anti-tick vaccine because it is potently immunogenic due to its numerous epitopes and a very high molecular mass. It consists of two monomers (KLH1 and KLH2) with 3400 amino acids that aggregate independently to yield very compact decameric and didecameric protein complexes [12, 13].

However, if we consider that an affordable veterinary vaccine for livestock requires a massive-scale and low-cost production [14], the evaluation of other highly immunogenic recombinant carrier proteins, cheaper than a natural protein such as KLH, should be explored for the development of an economically feasible anti-tick vaccine based on pP0 [15].

The dihydrolipoyl dehydrogenase protein (p64K) from the *Neisseria meningitidis* bacteria has been expressed with high yields in *Escherichia coli* [16]. This protein showed excellent properties as a carrier by enhancing immune responses against weak antigens [17], either through chemical conjugation [18–20] or by obtaining chimeric fusion recombinant proteins [21–23]. The presence of six free cysteine residues in p64K has never been explored before for chemical conjugation.

Considering that different synthetic strategies for chemical conjugation could yield striking differences in the physical, chemical, and biological properties of the resulting conjugates, the aim of this study was the synthesis, the SDS-PAGE analysis, the mass spectrometric characterization, and the immunogenicity and anti-tick efficacy evaluation of two chemical conjugates between pP0 and p64K that were named here as p64K-Cys^{1}pP0 and p64K-βAla^{1}pP0.

Materials and methods

Peptide synthesis

Two analogues of the peptide derived from the P0 acidic ribosomal protein of *Rhipicephalus* sp. ticks (pP0, NH$_2$–^{282}AAGGGAAAAKPEESKKEEAK^{301}–CONH$_2$) were synthesized [24]. The first analogue containing an intentionally added N-terminal Cys residue was named Cys^{1}pP0 (NH$_2$–^{1}CAAGGGAAAAKPEESKKEEAK^{21}–CONH$_2$). The second analogue has a β-Ala^1 residue as a spacer between a N-(β-maleimidopropionyl) group (Mal-) and the N-terminal end of pP0 (Mal-NH–^{1}(βA)AAGGGAAA AKPEESKKEEAK^{21}–CONH$_2$). Both pP0 analogues were purified by RP-HPLC and analyzed by ESI-MS.

Synthesis of pP0-p64K conjugates

The p64K (Q51225) from *N. meningitidis* produced in *E. coli* by the Center for Genetic Engineering and Biotechnology (batch number: 48.IFA.G812) was used in all experiments. The p64K-Cys^{1}pP0 conjugate was synthetized in two steps (Fig. 1a). Firstly, a reaction between p64K and N-(β-maleimidopropyloxy) succinimide ester (bmps), used as a cross-linking reagent, incorporates maleimide groups at Lys residues and the N-terminal end to yield an activated carrier protein. Briefly, the p64K dissolved at 1 mg/mL in 10 mM, pH = 6.0 in phosphate-buffered solution (PBS), reacted at a 1:5 ratio (w/w) with the cross-linker N-(β-maleimidopropyloxy) succinimide ester (bmps) that was previously dissolved in dimethylformamide (DMF) and stirred for 30 min at room temperature (RT). The reaction mixture was dialyzed against 10 mM PBS (pH = 6.0) at 4°C using a 30-kDa MWCO (Spectrapor, USA) membrane. In a second step (Fig. 1a), multiple copies of the Cys^{1}pP0 were added to the maleimide-activated p64K protein at a 1:1 ratio (w/w). The coupling reaction was gently stirred for 3 h at RT. The excess of peptide was eliminated by an overnight dialysis against the 10 mM, pH 7.2 phosphate-buffered solution at 4°C.

The p64K-βAla^{1}pP0 conjugate was synthesized in one step (Fig. 1b) by a reaction between the six free Cys residues of p64K and the Mal-βAla^{1}pP0. This peptide analogue and p64K solution were mixed in a molar ratio 5:1 in PBS containing 1 mol/L urea and the solution was gently stirred at RT for 12 h. The excess of peptide was separated from the conjugate by size exclusion chromatography (PD-10) previously equilibrated with 50 mM, pH = 7.4 PBS.
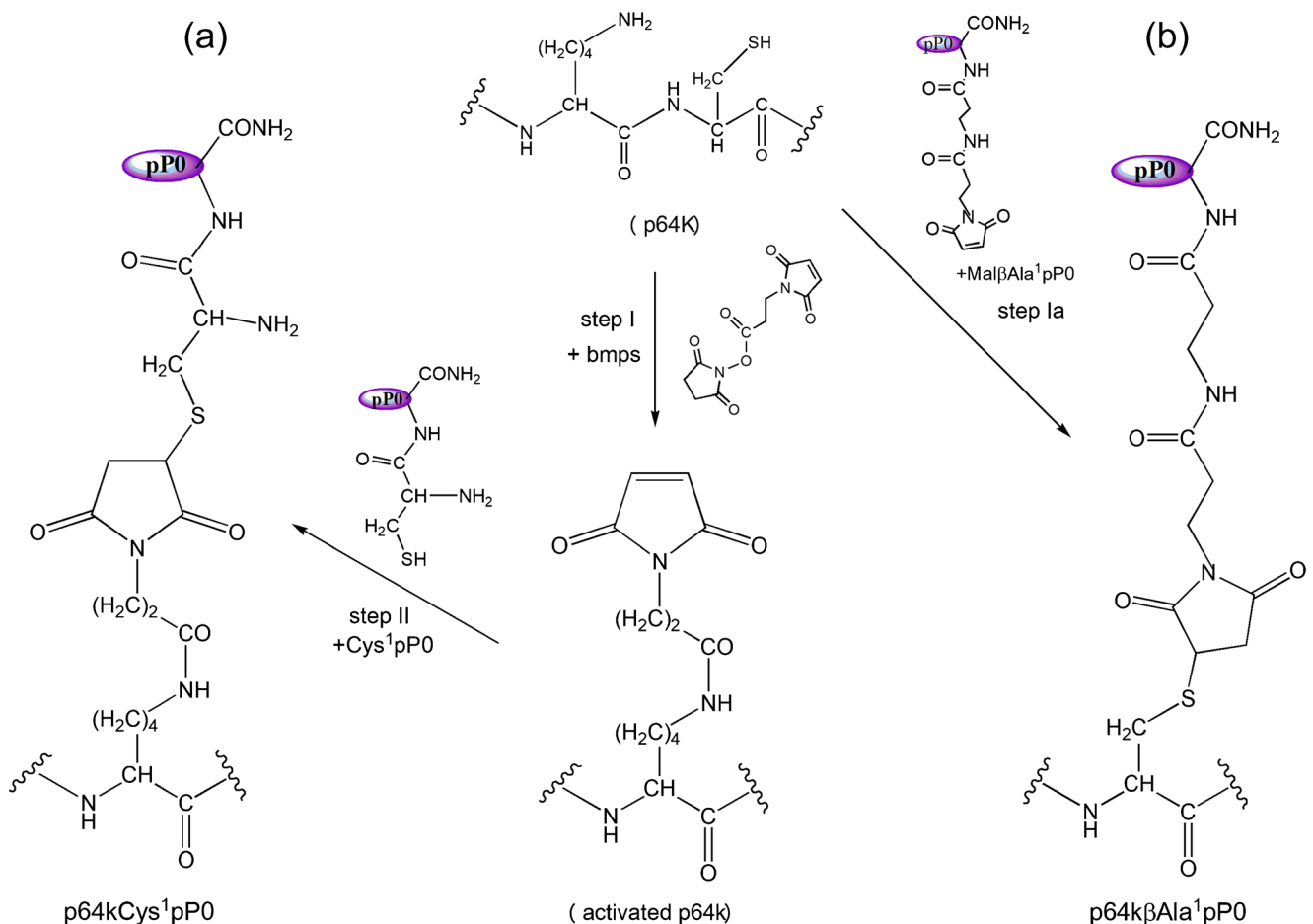
Fig. 1 Strategies for the synthesis of two vaccine candidates against ticks, here named p64K-Cys[1]pP0 (**a**) and p64K-βAla[1]pP0 (**b**). Both strategies are based on the chemical conjugation of the recombinant p64K carrier protein from *N. meningitidis* and two variants of a peptide from the tick acidic ribosomal P0 protein (Cys[1]-pP0 and Mal-βAla[1]-pP0) using the bmps as the heterobifunctional cross-linker reagent. Mal- means a maleimide group incorporated at the N-terminal end of the pP0 peptide during the solid-phase peptide synthesis. The ellipse indicates the sequence of the pP0 peptide (NH$_2$–[282]AAGGGAAAAKPEESKKEEAK[301]–CONH$_2$)

SDS-PAGE analysis of conjugates

Samples were separated in an 8% SDS-PAGE under reducing conditions [25]. Proteins were visualized with Coomassie blue R-250. Wide range molecular weight kit (Bio-Rad, USA) was used to estimate the protein molecular masses. The molecular masses of the synthetized conjugates as well as the carrier protein were determined by the Gel Analyzer free software available at http://www.gelanalyzer.com/.

Proteolytic digestion of conjugates

The p64K-Cys[1]pP0 conjugate dissolved at 5 mg/mL in a 1% ammonium bicarbonate solution, pH 8.3, was reduced with 10mM of DTT for 1 h at 37°C. The solution was cooled down to RT and free Cys residues were S-alkylated with 20mM of iodoacetamide for 30 min in the dark. The reduced and S-alkylated P64K-Cys[1]pP0 conjugate dissolved in a 1% ammonium bicarbonate solution, pH 8.3, was separately digested with LEP (Wako, Japan), trypsin (Promega), and V8 protease (Promega) for 4 h at 37°C using an enzyme-to-substrate ratio 1:100, 1:50, and 1:50, respectively. Half of the LEP and tryptic digestions were further digested in tandem with V8 protease in 1% ammonium bicarbonate solution, pH 8.3, for another 4 h at 37°C using 1:50 enzyme-to-substrate ratio. The conjugate p64K-βAla[1]pP0 was digested under the same conditions described above but it was not reduced and S-alkylated since all free cysteine residues were alkylated after the reaction with Mal-βAla[1]pP0. The mixture of peptides derived from all digestions (LEP, trypsin, V8, LEP+V8 and trypsin+V8) of both conjugates was acidified by adding 2 μL of 10 % formic acid and frozen at −20°C until LC-MS/MS analysis.

LC-MS/MS analyses

LC-MS/MS analyses of proteolytic peptides were performed using an UltiMate 3000 nano-HPLC system coupled to a QExactive Plus mass spectrometer equipped with an Easy-Spray source (Thermo Fisher Scientific, USA) as previously described [26]. LC-MS/MS analyses of proteolytic peptides were performed with an UltiMate 3000 HPLC system. Samples were loaded onto a pre-column (Acclaim PepMap™ 100, C18, 75μm × 2cm, 3-μm particle size) and separated with an Easy-Spray analytical column (PepMap™ RSLC, C18, 75μm × 50cm, 2-μm particle size) at 40°C. The column was equilibrated at 1% of buffer B (0.1% formic acid in acetonitrile) followed by an elution gradient from 1 to 55% of B over 70 min, 55 to 99% of B over 15 min, 99% of B for 5 min, and 1% of buffer A (0.1% of formic acid in water) for 15 min, with a constant flow rate of 200nL/min. The mass spectrometer was operated in a positive mode. Ion spray voltage was set at 2.5kV, capillary temperature at 250°C, and S-lens RF level at 50. Full MS scans were acquired in a range of 200–2000 m/z with a resolution of 70000 at 200 m/z, a AGC target value of $1×e^6$, and a maximum ion injection time of 100ms. Precursor fragmentation occurred in a HCD cell with a resolution of 17500 at 200 m/z, a AGC target value of $1e^5$, and a maximum ion injection time of 50ms. Normalized collision energy (nce) was used in a stepped mode (nce 25, 30, and 35). Precursor ions with single, unassigned, eight or higher charge states were excluded from analyses. A dynamic exclusion time was set to 30s.

Identification of conjugation sites based on the detection of type 2 peptides

Raw data or mgf files were loaded on pLink2 [27], Kojak [28], and StavroX [29] software. Two databases in the FASTA format containing the sequences of p64K and the corresponding pP0 analogues were created and queried for the identification of linear and type 2 peptides [30, 31]. The database used with Kojak software additionally contains the reverse sequences to determine the false discovery rate (FDR) through the Percolator software v 2.08 [32]. The elemental composition of the resultant linker ($C_7H_5O_3N$) was considered identical for the analysis of both conjugates. Nonetheless, the definition of the linked amino acids in type 2 peptides [30, 31] was different for the characterization of each conjugate (Cys-linker-Lys and Cys-linker-Nt for p64K-Cys[1]pP0 and only Cys-linker-Nt for p64K-βAla[1]pP0). Mass tolerance for the precursor and daughter ions was 10 ppm and 20 ppm, respectively. Deamidation of Asn and Gln residues as well as Met sulfoxide and S-alkylation of Cys residues with iodoacetamide were considered variable modifications. Three missed cleavage sites in the sequences of type 2 peptides, a 5% FDR and four amino acids, as the minimum length, were permitted for the

identification of type 2 peptides. The minimum and the maximum molecular masses of type 2 peptides were defined from 400 to 8,000 Da, respectively.

Side reactions of the linker [33] generated either during the synthesis, storage, and/or the proteolysis of the conjugates were determined by considering the chemical modifications in the linker and peptides, as well as the linked amino acids for each conjugate as shown in Electronic Supplementary Material (ESM) in Table S1a, Fig. S1a, S1b, and S1c (ESM can be downloaded from http://proteomics.fiocruz.br/ABC_manuscript).

Furthermore, the automatic assignments of type 2 peptides were manually validated by inspecting the presence of diagnostic ions in the MS/MS spectra (Fig. S2 in ESM). Peaks software [34] was used to identify dead-end peptides in p64K-Cys[1]pP0 by considering the increment in mass (+169.0375 Da) of cysteine residues due to the addition of N-maleimidyl propionic acid.

Retention time (rt) and experimental m/z values of the linear and type 2 peptides identified by the Kojak software with the precursor mass tolerance adjusted from 5 to 15 ppm were used to obtain the XICs with the Quin software (to appear at www.patternlabforproteomics.org).

Matrix-assisted laser desorption ionization mass spectrometry (MALDI-MS) analysis of the conjugates

Two percent acetic acid solutions of samples at a concentration of 1μg/μL were fivefold diluted with the same solution containing acetonitrile (2 %) and formic acid (0.3 %). A volume of 0.8 μL of the diluted samples was mixed on the MALDI plate with 0.5 μL of α-CHCA matrix prepared at 7 mg/mL in 50% acetonitrile solution containing 0.1 % of TFA. MALDI-MS analysis was carried out with a 4800 MALDI-TOF/TOF mass spectrometer (Applied Biosystems, Framingham, MA, USA). All mass spectra were obtained by averaging 2500 laser shots from each sample well in the linear mode. The entire process was controlled using 4000 series Explorer software (version 3.6, Applied Biosystems). Data were processed using Data Explorer software (version 4.8, Applied Biosystems).

Immunization and challenge experiments in rabbits

All procedures involving animals followed the Guide for the Care and Use of Laboratory Animals [35] and were approved by the Ethics Committee of the CIGB. Twelve F1 (New Zealand x White Semi Giant) young adult rabbits weighing from 1.8 to 2.3kg were obtained from the Center for the Production of Laboratory Animals (CENPALAB, Cuba) and were fed with a pelleted diet (produced by CENPALAB) and water *ad libitum* during the experiment. The trial was conducted in the Animal House at the CIGB. Four animals were

randomly selected for each of the three experimental groups. All groups were subcutaneously injected on days 0, 21, and 36. Groups 1 and 2 were immunized each time with 1mL/ rabbit containing 500μg of p64K-Cys^{1}pP0 and p64K-βAla^{1}pP0 conjugates in PBS, respectively, prepared in a 60/40 proportion of immunogen/water in oil adjuvant Montanide ISA 50 (SEPPIC, France). This adjuvant was included in the vaccine formulation as a delivery system in order to stimulate immune response by preserving the antigen conformational integrity and a slow release which improves the antigen presentation and to prolong its useful life [36, 37]. The negative control group only received PBS in the same oily formulation. Serum samples were taken on days 0, 21, 36, 50, and 125 to determine total IgG responses against pP0 and p64K using an indirect enzyme-linked immunosorbent assay (ELISA). Briefly, 100 ng per well of the pP0-KLH conjugate or p64K was used to coat ELISA plates overnight at 4°C. Plates were incubated with sera serially diluted 1:2 in PBS for 1h at 37°C and they were finally incubated with 1:10000 anti-rabbit IgG–HRP conjugate (Sigma) for 1h at 37°C. The staining reaction was developed with a substrate solution containing 0.4mg/mL of o-phenylenediamine in 0.1M citric acid and 0.2M Na_2HPO_4, pH 5.0, and 0.015% of hydrogen peroxide. The reaction was stopped with 2.5M H_2SO_4, and the OD490 nm was determined. Antibody titer was established as the reciprocal of the highest dilution, at which the mean OD of the sample serum was three times the mean OD of the negative control serum. Results were presented as the geometric mean of each group. The data were transformed using base 2 log to compare antibody titers between the two immunized groups with t-tests performed on Prism (version 6.0 for Windows; GraphPad Software, USA).

On day 60, each rabbit was challenged with 250±25 larvae, 200±15 nymphs, and 50 adults (25 female and 25 male ticks) of *R. sanguineus* ticks from a tropical lineage maintained at the CIGB [38] using craft feeding chambers glued to its shaved flanks [39]. The number of all fed-tick stages collected was recorded and they were kept in an incubator at 28± 2°C with 80% relative humidity, and a photoperiod of 12h of light. Fed larvae and nymphs were stored in daily batches and mortality during the molting period was also recorded. Detached fully engorged females were placed in individual glass vials during oviposition. Egg masses were individually weighed and incubated to determine hatchability by visual observation [40]. Group averages for each measured parameter were compared by ANOVA and Bonferroni multiple comparisons' test performed on Prism (version 6.0 for Windows; GraphPad Software, USA). The overall efficacy of each antigen (E) was calculated by including the effects on each tick stage as $E = 100 \times (1 - [RL \times VL \times RN \times VN \times RA \times PA \times FE])$ where RL and VL represent the effects of each immunogen on larvae yield and viability in the molting process compared to the control group. RN and VN are the effects of each immunogen

on nymph yield and viability in the molting process compared to the control group. RA and PA are the effects of each immunogen on female recovery and oviposition compared to the control group. FE is the effect of each immunogen on egg fertility. It was calculated as the ratio between the hatching percentages of eggs laid by ticks fed on vaccinated animals compared to the control group. Parameters in the vaccinated groups that were not statistically different to those of the control group were not considered when calculating efficacy [15].

After challenge, peripheral blood mononuclear cells (PBMCs) from three rabbits for each group were isolated by Histopaque (Sigma, USA) centrifugation and cultured in 24-well culture plates using apyrogenic RPMI 1640 medium supplemented with 2 mM L-glutamine, 10 mM HEPES, 1× Antibiotic Antimycotic Solution, and 10 % FCS. Twelve wells with one million of each PBMC sample were seeded. Four wells were stimulated with 6 mg/mL of the KLH-Cys^{1}pP0 conjugate or with Concanavalin A (Sigma, USA) as a positive control. The remaining four wells were cultivated without any stimulation as a negative control. After 24 h and 48 h of incubation to 37°C with atmosphere of 5% CO_2, cells from two wells for each culture condition were collected by centrifugation and total RNA was purified by using Tri-reagent (Sigma) as recommended by the manufacturer. Previous to the cDNA synthesis performed with Superscript III First-Strand Synthesis System (Invitrogen) and random primers, all RNA samples were treated with DNAse-RNAse free (Invitrogen). Quantitative real-time PCR was performed by using a Rotor-Gene 3000 Detection System (Corbett, Life Science). Briefly, 5 μL of each template cDNA was mixed with 6.5 μL of 2× SYBR Green PCR master mix (Quantitect SYBR Green PCR kit, Qiagen, USA) and 0.3 μM of forward and reverse primers in a final volume of 12.5 μL. Specific primers are summarized in Table S1b (see ESM) [41]. The amplification program was 15 min at 95°C and 45 cycles of 15 s at 95°C, 20 s at 60°C, and 15 s at 72°C. All reactions were run in duplicate. For gene expression quantification, the comparative Ct method was used. First, gene expression levels for each sample were normalized to the expression level of the housekeeping gene encoding glyceraldehyde 3-phosphate dehydrogenase (GAPDH) (ΔCt sample = Ct specific gene − Ct GAPDH). The difference between each PMBC sample stimulated with antigen compared to non-stimulated same sample was used to calculate the $\Delta\Delta$Ct (ΔCt sample stimulated − ΔCt sample non-stimulated). The $2^{(-\Delta\Delta Ct)}$ comparison gave the relative fold change in gene expression of the vaccinated versus non-vaccinated animals ($2^{(-\Delta\Delta Ct)}$ vacc/$2^{(-\Delta\Delta Ct)}$ non-vacc). Statistical significance of the fold change between samples was calculated with the Wilcoxon signed-rank test performed on Prism (version 6.0 for Windows; GraphPad Software, USA).

Results and discussion

SDS-PAGE and MALDI-MS analysis of p64K-Cys[1]pP0 and p64K-βAla[1]pP0 conjugates

p64K-Cys[1]pP0

The SDS-PAGE analysis of the p64K carrier protein showed a single band estimated at a molecular mass of 76 kDa (Fig. 2a, lane 2), which is considerably higher than the expected 62,006.17 Da, according to the amino acid sequence deduced from its cDNA sequence. This abnormal migration in SDS-PAGE could be attributed to a gel shifting phenomenon [42] because the ESI-MS analysis showed an agreement between the experimental (62,006.00 Da) and the expected molecular masses of the intact p64K (see in ESM, Fig. S3a, S3b). Furthermore, the LC-MS/MS analysis of all proteolytic digestions of p64K-Cys[1]pP0 and p64K-βAla[1]pP0 conjugates enabled the verification of 100% and 99.7% of the p64K sequence, respectively (see in ESM, Fig. S3c, d). The p64K-Cys[1]pP0 conjugate migrated as a diffused and broad band between 78 and 104 kDa, indicating its heterogeneity in size (Fig. 2a, lane 3 and Fig. S3e). These results are expected for a non-site-specific synthetic procedure targeting all primary amino groups of p64K exposed on the protein surface [15]. Moreover, a second broad band observed in the SDS-PAGE analysis of p64K-Cys[1]pP0 between 157 and 223 kDa and other upper bands (MW > 240kDa) suggested conjugate multimerization (Fig. 2a, lane 3) by the cross-linking agent (bmps), because it could cross-link not only Cys[1]pP0 to the carrier protein but also two or more molecules of p64K or its resultant conjugate through intermolecular linkage between free cysteine and Lys residues. Previous cross-linking experiments of p64K and EGS and size exclusion chromatography demonstrated that this protein in solution is a dimer [43] and a tetramer like other dehydrogenases [44]. The densitogram of p64K-Cys[1]pP0 separated by SDS-PAGE (Fig. 2a, lane 3) revealed that the bands assigned to monomer (78–104 kDa), dimer (157-223 kDa), and multimers (MW >240kDa) represent approximately 43.9%, 45.5%, and 10.5% of the integrated area, respectively (Fig. S3e in ESM). These cross-linked aggregates were exclusively observed in the SDS-PAGE analysis under reducing conditions for p64K-Cys[1]pP0 (Fig. 2a, lane 3). Wakankar and coworkers observed in the production of antibody-drug conjugates that intermediates containing free cysteine residues and maleimido groups aggregate via intermolecular cross-linking and are less stable than the resultant conjugates [45].

The molecular mass of the p64K-Cys[1]pP0 conjugate (Fig. 2b) was determined by MALDI-MS analysis for an accurate calculation of the Cys[1]pP0/p64K ratio. The unknown magnitude of the gel shifting phenomenon for p64K-Cys[1]pP0 does not allow a precise determination of this ratio by SDS-PAGE

analysis. The cluster of signals observed around 71 and 35 kDa corresponded to $(M+H)^+$ and $(M+2H)^{2+}$ ions of p64K-Cys[1]pP0, respectively (Fig. 2b). Each signal in both clusters was equally spaced by approximately 2.1 kDa which is in agreement with the several additions of Mal+Cys[1]pP0 units (2.152 kDa each) to Lys residues of the carrier protein. It should be noted that the difference (2743.4 Da) in mass between 64749.4 (the lowest mass of the cluster) and 62006 (the observed molecular mass for the intact p64K in Fig. S3) was higher than the calculated Mal-Cys[1]pP0 mass (2152.02 Da) by 591.4 Da.

Considering the accuracy and resolution of a measurement performed by MALDI-MS analysis in linear mode, this mass difference (+591.4 Da) was agreeable with the sum of four β-maleimidopropyloxy moieties (604 Da =4 × 151 Da) after linking intra-molecularly four Cys to nearby Lys residues in p64K by bmps. Supposing this side reaction partially occurred in step 1 prior to the addition of Cys[1]pP0 (Fig. 1a), the observed signals in Fig. 2b separated by 2.1 kDa could be assigned to the conjugate linked from one to eight Cys[1]pP0 peptides per p64K, among which three to five additions of Cys[1]pP0 were the most abundant species.

Kojak and plink2 software assigned 73 MS/MS spectra to sixty-two [p64K]-[p64K] type 2 peptides (Table S5h and Fig. S18) with the intact and the hydrolyzed linker [33]. This result could also explain the increment in the molecular mass (+590 Da) of the monomeric form of p64K-Cys[1]p0 in MALDI-MS analysis (Fig. 2b) and, at the same time, the presence of dimer and multimers in p64K-Cys[1]p0 (Fig. 2a, lane 3) if Cys and Lys resides were linked by bmps in an intra- or intermolecularly way, respectively.

Immunological identification using Western blot analysis with purified anti-pP0 polyclonal antibodies (Fig. S4a) and the anti-p64K monoclonal antibody (Fig. S4b) confirmed that all bands observed in SDS-PAGE (Fig. 2a, lane 3) corresponded to the p64K-Cys[1]pP0 conjugate and its covalent multimers.

p64K-βAla[1]pP0

The p64K-βAla[1]pP0 conjugate was highly homogeneous in size and migrated as a very well-defined band at 91 kDa on the SDS-PAGE analysis (Fig. 2a, lane 4). Western blot analyses using the same antibodies mentioned above demonstrated the identity of the 91-kDa band as the p64K-βAla[1]pP0 conjugate (Fig. S4a and S4b). Urea was included in the reaction buffer at a final concentration of 1mol/L to equalize the accessibility of the free Cys residues in p64K; otherwise, heterogeneity of the conjugate becomes clearly observed in SDS-PAGE analysis (see in ESM Fig.S4c). The fully reduced and carbamidomethylated p64K and the recombinant streptokinase (a protein devoid of Cys residues) did not increase their molecular masses after treatment with Mal-βAla[1]pP0 (in ESM Fig. S4d). Broad protein bands such as the observed for p64K-Cys[1]pP0 typical
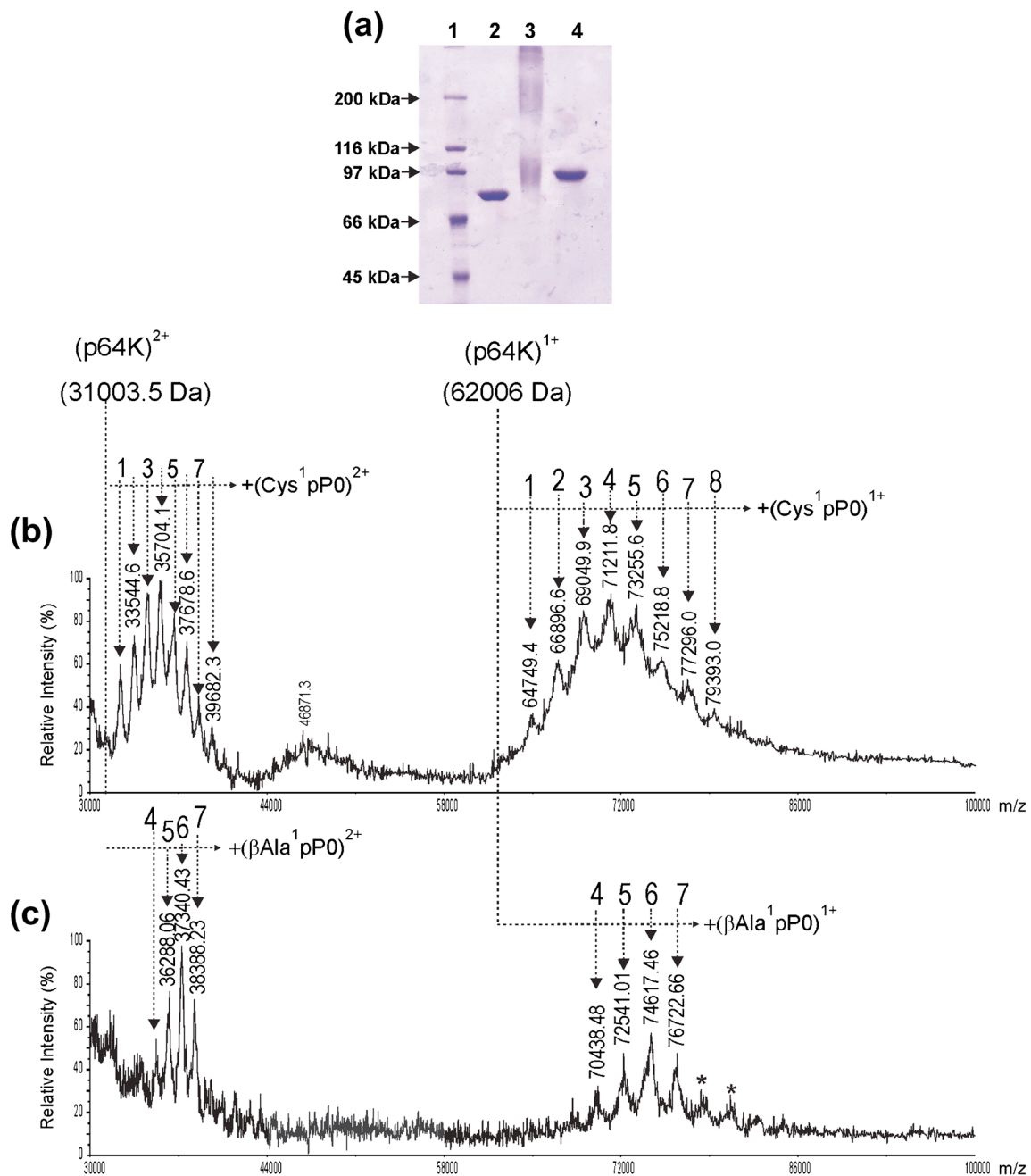
Fig. 2 (**a**) SDS-PAGE analysis under reducing conditions of the synthetized conjugates p64K-Cys[1]pP0 and p64K-βAla[1]pP0. Lane 1: molecular weight markers; lane 2: recombinant p64K carrier protein from *N. meningitidis*; lane 3: p64K-Cys[1]pP0; and lane 4: p64K-βAla[1]pP0. The MALDI-MS spectra shown in (**b**) and (**c**) correspond to the p64K-Cys[1]pP0 and p64K-βAla[1]pP0, respectively. The broken lines indicate the additions of several units of Cys[1]pP0 and βAla[1]pP0 to the p64K protein in the resultant conjugates. The number of units of pP0 (1-8) added in the resultant conjugates are indicated above each signals. +(Cys[1]pP0)[1+] and +(Cys[1]pP0)[2+] correspond to singly and doubly charged ions of p64K-Cys[1]pP0, while +(βAla[1]pP0)[1+] and +(βAla[1]pP0)[2+] correspond to the same information for p64K-βAla[1]pP0. Asterisks in (c) correspond to probably further additions (8-9) of βAla[1]pP0 to the amino groups of p64K carrier protein

for non-specific chemical reactions targeting many Lys residues exposed on the protein surface were not observed. The results obtained by SDS-PAGE suggested that the reaction proceeded through the free thiol groups [46].

Considering the limitations of SDS-PAGE analysis for determining accurate molecular mass of p64K-βAla[1]pP0 due to the gel shifting phenomenon, the βAla[1]pP0/p64K molar ratio was determined by MALDI-MS. Similar to the case of p64K-

Cys[1]pP0, the cluster of ion signals was observed around 37 and 74 kDa, which corresponded to $(M+2H)^{2+}$ and $(M+H)^+$ ions of the p64K-βAla[1]pP0, respectively (Fig. 2c). The signals on both clusters were almost equally spaced (2.1 kDa), indicating that the heterogeneous number of Mal-βAla[1]pP0 (2120.05 Da) was linked to p64K. These results showed that p64K-βAla[1]pP0 was also a heterogeneous conjugate despite of the homogeneous band observed on the SDS-PAGE analysis, but this heterogeneity was definitively lower than the observed for p64K-Cys[1]pP0.

The mass difference (12611 Da) between the intact p64K (62006 Da) and the most intense signal (74617 Da) observed in the MALDI-MS spectrum (Fig. 2b) corresponds to a βAla[1]pP0/p64K ratio of 5.95 in the analyzed conjugate. This value is close to the expected addition of six βAla[1]pP0 units considering that p64K carries six free Cys residues [16, 47]. Therefore, other signals detected at 72.5 kDa and 76.7 kDa sharing similar intensity in the MALDI-MS spectrum (Fig. 2c) were assigned to the addition of 5 and 7 units of βAla[1]pP0 to the carrier protein.

The MALDI-MS analysis (Fig. 2c) showed that p64K-βAla[1]pP0 is linked to 4–5 units of βAla[1]pP0. We hypothesized that during p64K denaturation and overnight reaction with Mal-βAla[1]pP0, some of its six free cysteine residues would be partially involved in the formation of new disulfide bonds different to the present in the native p64K [47, 48]. pLink2 software [27] assigned sixteen high-quality MS/MS spectra to five disulfide-bridged peptides (see Table S5, and Table S5j and Fig. S20), different to the expected between Cys[157] and Cys[162]. The formation of extra disulfide bonds in p64K not only increased the heterogeneity observed in MALDI-MS analysis (Fig. 2c) of p64K-βAla[1]pP0, but also diminished the βAla[1]pP0/p64K ratio, a very important aspect for the biological activity of conjugates.

The MALDI-MS analysis of p64K-βAla[1]pP0 showed additions of 7–9 βAla[1]pP0 units higher than the expected of six (Fig. 2c). Although maleimide is 1000 times more selective by thiols over amino groups [49], there are reports related with the reactivity of maleimide towards the primary amino groups [50]. The pLink2 [27] and Kojak [28] software assigned forty-five type 2 peptides linked by bmps through their primary amino groups and they were supported by fifty-one high-quality MS/MS spectra (see Table S5, and Table S5i and Fig. S19). Also most of these type 2 peptides were also detected with a hydrolyzed linker as described previously [33]. The reaction of Mal-βAla[1]pP0 with primary amino groups in p64K increased the payload at expenses of an undesirable loss of the homogeneity of the conjugate although not at the extent observed for p64K-Cys[1]pP0. These results demonstrate the necessity of applying orthogonal techniques in order to characterize the homogeneity of the synthetized conjugates.

## Identification of the conjugation sites of p64K-Cys[1]pP0 and p64K-βAla[1]pP0 by LC-MS/MS analysis

p64k-Cys[1]pP0

The software Kojak [28], StavroX [29], and pLink2 [27] assigned 350, 252, and 340 MS/MS spectra to type 2 peptides, respectively (Fig. 3a) in which two independent peptides' chains belonging to p64K protein and pP0 peptide were cross-linked. The number of conjugation sites assigned by the individual software was very similar (Fig. 3a). The Kojak and StavroX software identified the same set of conjugation sites (36 in total) while pLink2 assigned 34. No conjugation site was exclusively assigned by a single software. Ninety-four percent of the conjugation sites (34/36) were coincidently assigned by the three evaluated software. This appreciable redundancy suggests reliable results considering that used software is based on different scoring methods and algorithms. Summarizing, thirty-five Lys residues and the N-terminal end of p64K were found to be partially conjugated to Cys[1]pP0. Only four Lys residues, located at positions 446, 563, 594, and 595 in the p64K sequence, were found unmodified (Fig. S3c).

The Venn diagram showing the overlapping results in the assignment of the MS/MS spectra to type 2 peptides (Fig. 3b) indicated that almost 30% of the MS/MS spectra assigned to type 2 peptides were coincidently identified by the three software. Close to 20% were assigned by using at least two software, and 44.9 % were exclusively identified by only one software. This result shows a great complementarity and reinforces the importance of using several software to analyze the proteolytic digestions of the conjugates; otherwise, the number of MS/MS spectra assigned to type 2 peptides could be considerably underestimated. Complementary results have previously been well documented when the same dataset is analyzed by different software developed to identify type 2 peptides [28, 51, 52]. Table S2 summarizes the conjugation site assignments based on the identification of 510 MS/MS spectra corresponding to type 2 peptides derived from p64K-Cys[1]pP0. All MS/MS spectra assigned to type 2 peptides by pLink2 [27], Kojak [28], and StavroX [29] are shown in Fig. S5, S6, and S7, respectively. The numbers of type 2 peptides and MS/MS spectra that support the assignment of the individual conjugation sites in p64K-Cys[1]pP0 are summarized in Fig. S8a.

The automatic identification of type 2 peptides was manually validated by considering the presence of diagnostic ions in their corresponding MS/MS spectra (Fig. S2). Some of these fragment ions revealed the size of Cys[1]pP0 in the type 2 peptides, as shown in a previous manuscript [15]. In particular, the presence of a proline residue in the sequence of pP0 yields a very favorable fragmentation (y''_n ion) of the peptide bond at the N-terminal end of proline [53] that can be very
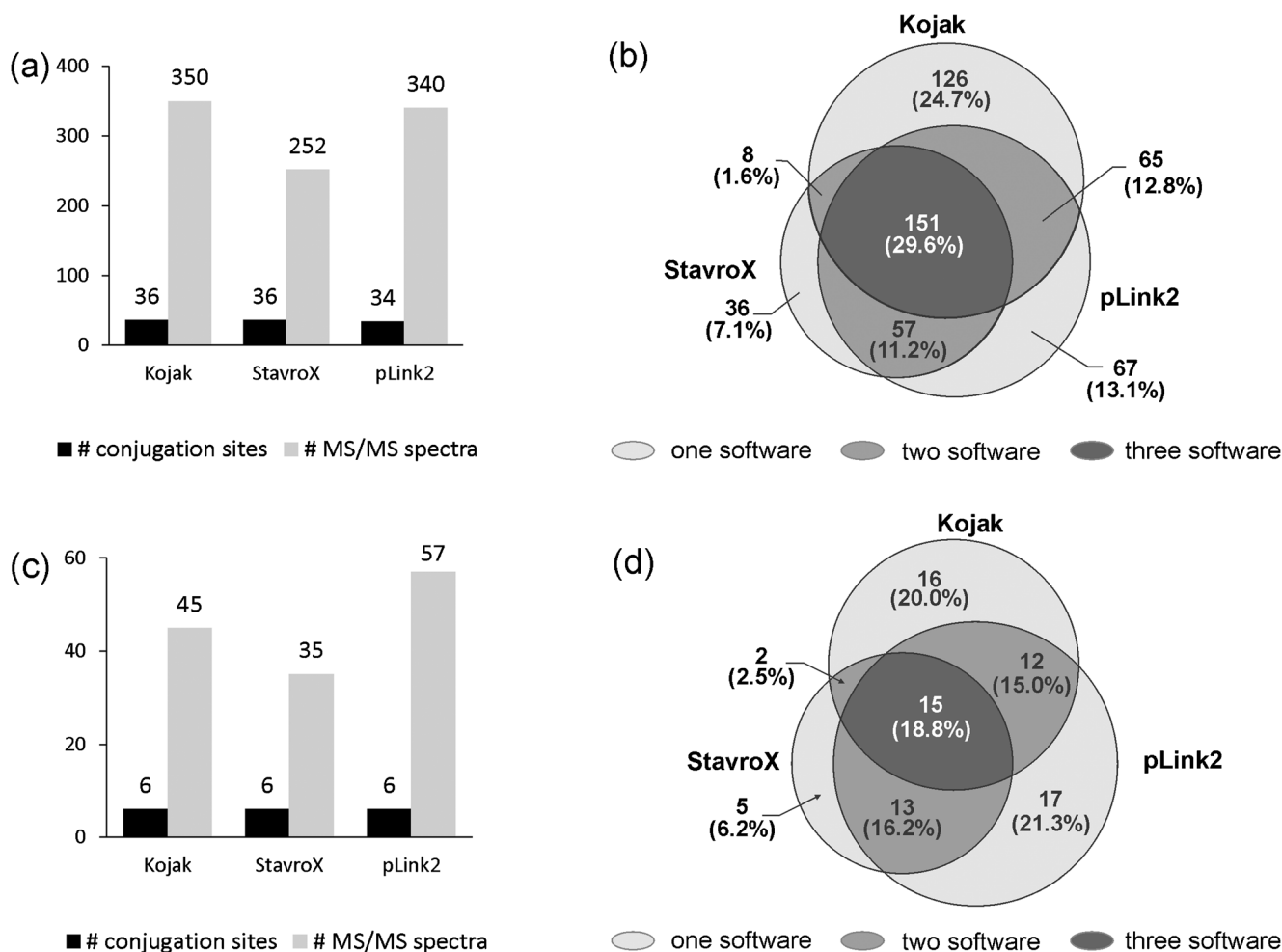
Fig. 3 (**a**) Conjugation site assignment in p64K-Cys[1]pP0. Dark- and gray-solid bars indicate the number of conjugation sites and their corresponding MS/MS spectra assigned to type 2 peptides by the evaluated software (Kojak [28], StavroX [29], and pLink2 [27]), respectively. (**b**) The Venn diagram shows the overlapping results of the evaluated software for the assignment of MS/MS spectra to type 2 peptides containing the conjugation sites in p64K-Cys[1]pP0. (**c**) Conjugation site assignments in p64K-βAla[1]pP0. Light-gray bars indicate the number of MS/MS spectra assigned by software to type 2 peptides containing the conjugation sites. Dark bars indicate the number of conjugation sites identified by the evaluated software in p64K-βAla[1]pP0. (**d**) The Venn diagram with overlapping MS/MS spectra assigned to intermolecular type 2 peptides by the evaluated software. The shaded areas in both Venn diagrams are labeled with the number of MS/MS spectra assigned to type 2 peptides as well as the percentage they represent

useful for validation purposes. For example, in the MS/MS spectrum of a type 2 peptide composed by [Ile[257]-Arg[271]] of p64K linked through the Lys[262] to the thiol group of Cys[1]pP0 [1–16], a very intense fragment ion observed at m/z 589.28 was assigned to y″$_{5\beta}$ (Fig. 4a).

Approximately, 98% of type 2 peptides generated by either trypsin or Lys-C cleavages were detected with $Z \geq 3+$ (Table S2, and S4 in ESM). This result agrees with previous reports [54] and confirms that the manual validation of the data was reliable for the assignment of the conjugation sites. A more detailed analysis for the charge-state distribution of all type 2 peptides is shown in Fig. S13a and S13c (see ESM). The manual validation process although time consuming was essential for obtaining reliable results in the identification of the conjugation sites.

The pLink2 [27] and Kojak [28] software assigned 98 MS/MS spectra to 75 type 2 peptides with hydrolyzed linker (see Table S5 and Fig. S13a). The generation of these type 2 peptides was probably favored during proteolysis at basic pH [33]. Although it did not contribute to the identification of new conjugations sites, the number of assigned MS/MS spectra increased considerably and it had a favorable impact in the reliability of the results. Other side reactions associated with the synthesis of p64K-Cys[1]pP0 are summarized in Table S5.

The extracted ion chromatograms (XICs) corresponding to type 2 peptides derived from different proteolytic digestions also reflected the heterogeneity of p64K-Cys[1]pP0 conjugate. The XICs of type 2 peptides obtained for the trypsin+V8 digestion showed similar number of fractions to those obtained
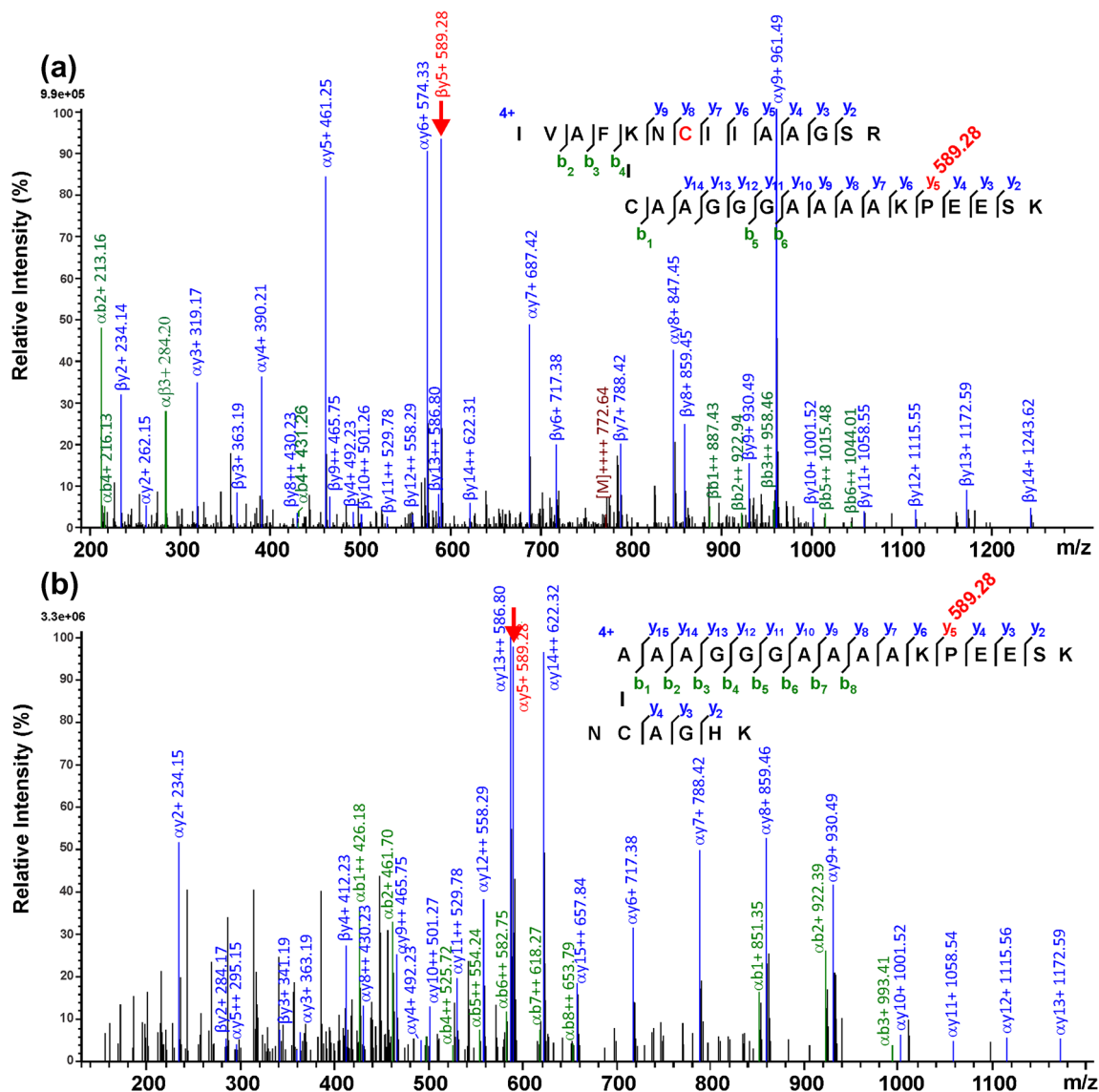
Fig. 4 (**a**) MS/MS spectrum assigned by pLink2 software to a type 2 peptide (*m/z* 772.6390, 4+) in p64K-Cys^{1}pP0 composed by a proteolytic peptide of p64K [258-271] linked through the side chain of K262 to Cys^{1}pP0(1-16). "C" in red means carbamidomethyl Cys residue. (**b**) The MS/MS spectrum of a signal detected at *m/z* 542.0011, 4+ assigned by pLink2 to a type 2 peptide [457-462]-βAla^{1}pP0 (1-16) containing the Cys^{458} as a conjugation site in p64K. The solid arrows shown in the MS/MS spectra of [258-271]-Cys^{1}pP0 (1-16) (**a**) and [457-462]-βAla^{1}pP0(1-16) (**b**) were assigned as y"$_{5\beta}$ and y"$_{5\alpha}$, respectively, and they correspond to a diagnostic ion (*m/z* =589.283)

for linear peptides (see in ESM Fig. S9a, Table S3a and Fig. S9b, Table S3b) for two reasons: (1) 35 out of the 39 Lys residues and the N-terminal end were partially linked to Cys^{1}pP0 and (2) all type 2 peptides containing the same conjugation site were in general heterogeneous regarding the size of the Cys^{1}P0 peptide linked in their structures because proteases cleave at different positions, aspect that can be more noticeable in the tandem digestions. Thirty-eight type 2 peptides with twenty-five different conjugation sites were identified in the LC-MS/MS analysis of the trypsin+V8 tandem digestion (Fig. S9b, Table S3b in ESM).

The area under the curve for the individual XICs suggested the coexistence in the analyzed sample of type 2 peptides of remarkably different abundances. This result suggests that a sensitive LC-MS/MS analysis covering a wide dynamic concentration range is needed for the characterization of conjugates synthesized by a non-site-directed approach; otherwise, the number of conjugation sites can be underestimated. The XICs of linear and type 2 peptides of the synthetized conjugates were also useful to evaluate the batch-to-batch reproducibility (data not shown).

The high heterogeneity of p64K-Cys^{1}pP0 verified by SDS-PAGE (Fig. 2a, lane 3), MALDI-MS (Fig. 2b), and LC-MS/MS (Fig. S9a-S9b) analyses agreed with a non-site-specific conjugation approach targeting most of the exposed Lys residues.

p64K-βAla^{1}pP0

The LC-MS/MS analyses of all proteolytic digestions derived from p64K-βAla^{1}pP0 conjugate enabled the identification of all the expected conjugation sites at the six free Cys residues (264, 458, 515, 549, 556, and 586) in the p64K sequence. The three software were fully coincident in this assignment (Fig. 3c and Table S4 in ESM). Eighty-one MS/MS spectra were assigned to type 2 peptides considering the contribution of the three evaluated software (Table S4, Fig. S10, S11 and S12 in ESM). Kojak, StavroX, and pLink2 software assigned 45, 35, and 57 MS/MS spectra to type 2 peptides (Fig. 3c), respectively.

As shown in the Venn diagram, less than 20% of these MS/MS spectra were coincidently assigned to type 2 peptides by the three software (Kojak, pLink2, and StavroX) (Fig. 3d), and approximately 34% when the combination of two software were considered. Approximately 47% of all MS/MS spectra were assigned to type 2 peptides by the exclusive contribution of the individual software. The numbers of type 2 peptides and MS/MS spectra that support the assignments of the individual conjugation sites in p64K-βAla^{1}pP0 conjugate by each software are summarized in Fig. S8b and S8c. The pLink2 [27] and Kojak [28] software assigned 95 MS/MS spectra to 54 type 2 peptides with hydrolyzed linker (see Table S5, Table S5b, and Fig. S13b). This result contributed to the reliability of the results because it increased considerably the number of supporting MS/MS spectra and also a pattern of signals separated by 18 Da in the ESI-MS spectra corresponded mostly to the same type 2 peptide with the intact and hydrolyzed linker [33]. Other side reactions associated with the synthesis of p64K-βAla^{1}pP0 are summarized in Table S5.

Figure 4b shows a MS/MS spectrum assigned to a type 2 peptide [457-462]-βAla^{1}pP0(1-16) containing the conjugation site at C458. In addition, the peptide [457-462] assigned as beta peptide [31, 55], with a short-length sequence of 6-amino acid residues, is represented in the MS/MS spectrum by only three consecutive y"$_n$ ions series (y"$_{2\beta}$, y"$_{3\beta}$, and y"$_{4\beta}$). The intense fragment ion detected at m/z 589.283 in Fig. 4c indicates that peptide [457-462] is linked to βAla^{1}pP0 (1-16) . This type 2 peptide was correctly assigned by the pLink2 and Kojak software.

In agreement with previous reports in literature [55], all type 2 peptides with Lys and/or Arg at their C-terminal ends in p64K-βAla^{1}pP0 were detected with $Z \geq 3+$ (Table S2, S4, and Fig. S13b abs S13d, see ESM). Type 2 peptides with $Z=2+$ were mainly generated by tandem digestions (LEP+V8 and trypsin+V8) and had Asp/Glu at their C-termini. Although they represented a minority fraction of all identifications, they were not automatically excluded from the LC-MS/MS analysis [55, 56] because they contributed decisively to identify two nearby conjugation sites (C549 and C556) in

two separated type 2 peptides in p64K-βAla^{1}pP0. It also suggests that the identification of higher order peptides [30, 31] containing several conjugation sites is not favored either because their high molecular masses are not efficiently fragmented by HCD [55] and in consequence they are not identified or simply because the software is not able to assign MS/MS spectra with such complexity.

Tandem digestions (trypsin+v8 and LEP+v8) allowed the identification of some conjugation sites that were not identified when only LEP and/or trypsin was used. Tandem digestions transformed high molecular mass type 2 peptides into peptide species with an optimal size to be fragmented efficiently by HCD and it partially compensates the limitation of using only one fragmentation method. The LC-MS/MS analysis of several proteolytic digests of the conjugates was essential for a wide coverage and reliable assignment of the conjugation sites; otherwise, they might be underestimated.

All the results shown in this manuscript were obtained after manual validation of the output with an FDR $\leq 5\%$ and considering the presence of the diagnostic ions in the MS/MS spectra. This aspect is time consuming and undoubtedly is the bottleneck in the workflow analysis of both conjugates (Table S2 and S4). Output with an FDR $\leq 1\%$ facilitates the manual validation process because a considerably lower number of MS/MS spectra need to be manually inspected. However, in our experience, several MS/MS spectra contained in the 1% $<$FDR $\leq 5\%$ output have enough quality to be considered as positive identifications and, at the same time, they may contain useful information for the characterization of the conjugation sites. It is important to point out that if FDR $\leq 1\%$ is the choice defined by the user, MS/MS spectra should be inspected anyway because some of them may not satisfy the manual validation process.

The extracted ion chromatograms corresponding to linear (see Fig. S9c) and type 2 peptides (see Fig. S9d) derived from the trypsin+V8 digestion of p64K-βAla^{1}pP0 showed 32 and 6 fractions, respectively. The XIC was very simple showing only six different type 2 peptides containing four conjugation sites (Fig. S9d, Table S3c in ESM). The results shown here confirm that p64K-βAla^{1}pP0 is a conjugate more homogeneous than p64K-Cys^{1}pP0.

Efficacy of p64K-Cys^{1}pP0 and p64K-βAla^{1}pP0 conjugates

Rabbits immunized with both conjugates showed similar antibody responses against p64K (Fig. 5a). However, the specific antibody titers against pP0 were statistically higher in the group immunized with p64K-Cys^{1}pP0 than in the group immunized with p64K-βAla^{1}pP0 on days 36 and 51 (Fig. 5a). Quantitative analysis of common cytokines expressed by peripheral blood mononuclear cells (PMBCs) of immunized rabbits after "in vitro" stimulation with the vaccine antigen
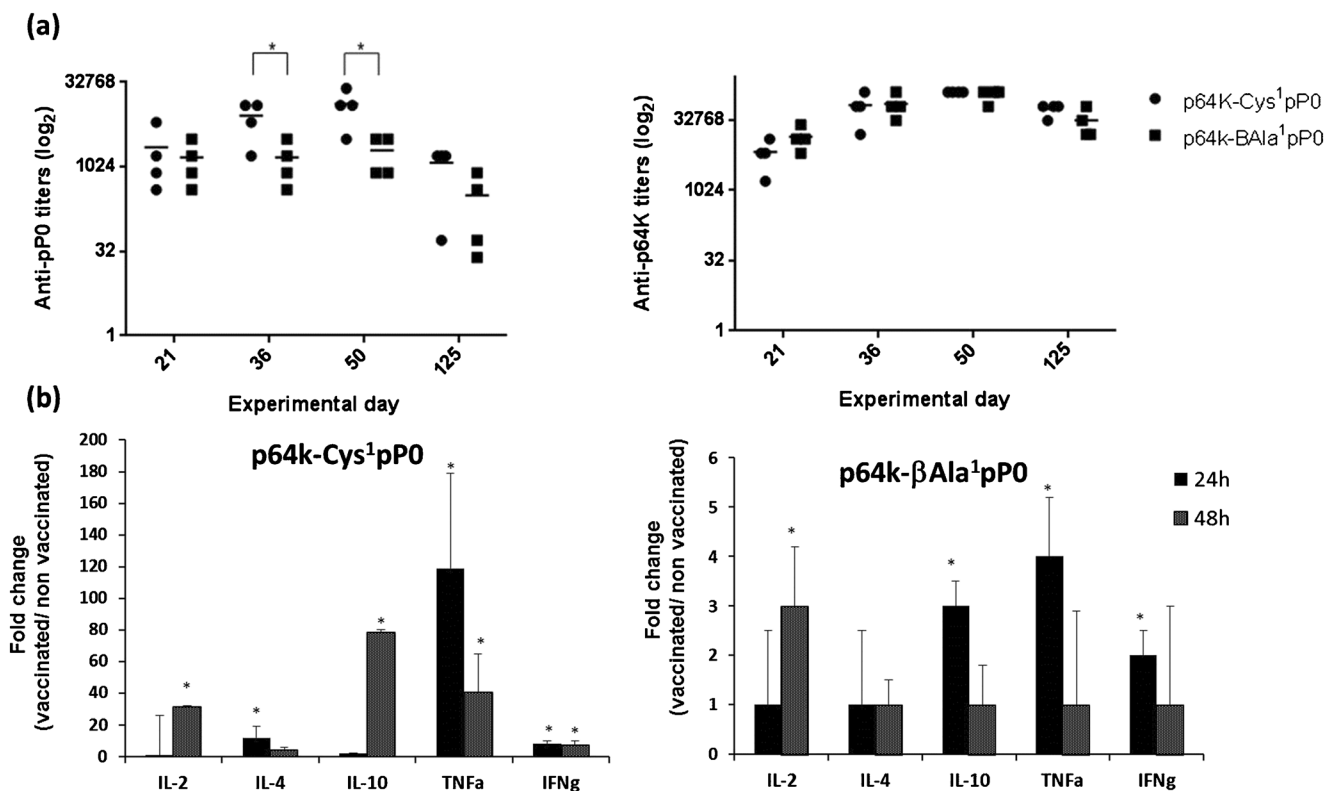
Fig. 5 (**a**) Specific antibody responses obtained in immunized rabbits against pP0 and p64K. The *Y* axes are in a logarithmic scale. Each point represents the antibody titer of one animal inside the group and the line represents the geometric mean of antibody titers in the group. Asterisks represent statistically significant differences in the antibody titers between immunized groups (*t*-test, *P<0.05). (**b**) Fold change of cytokine expression in PBMCs of vaccinated rabbits over non-vaccinated rabbits. Asterisks represent statistical significance (*p*-value) calculated using the Wilcoxon signed-rank test (*P<0.05)

showed a pattern of mixed Th1/Th2 response in both groups but with a higher magnitude in the group immunized with p64K-Cys[1]pP0 than in the group immunized with p64K-βAla[1]pP0 (Fig. 5b). A significant increase in the expression of IL-2, TNFα, and IFNγ was obtained for both groups, which are pro-inflammatory cytokines of a Th1 expression profile. In addition, IL-4 and IL-10 expressions were also significantly increased. These cytokines are considered anti-inflammatory and tend to modulate host immune responses away from a Th1 profile and towards a Th2 phenotype. The modulation of host immunity by tick saliva is of major importance in the successful accomplishment of the blood meal. It is known that many tick species preferentially induce host Th2 lymphocyte responses [57]. However, the resistance to tick infestation is due to a complex set of responses, and its specific mechanisms and their relative importance continue to be largely unknown but IL10 appears to be associated with long-term tick resistance [58].

Accordingly, the overall calculated efficacy against *R. sanguineus* ticks was 81% and 45% for p64K-Cys[1]pP0 and p64K-βAla[1]pP0, respectively (Table 1). This result agrees with the correlation previously demonstrated between antibody titers against pP0 and anti-tick efficacy [15]. The group immunized with p64K-Cys[1]pP0 showed statistically

significant differences with the control group in larvae recovery and viability, nymph viability, and egg hatchability. In the group immunized with p64K-βAla[1]pP0, statistical differences were only observed in nymph recovery and egg hatchability (Table 1).

Summarizing, the best immune response against pP0 obtained with the highly heterogenous p64K-Cys[1]pP0 conjugate implied the highest efficacy against *Rhipicephalus sanguineus* ticks, when immunized rabbits were simultaneously challenged with the three life stages of this tick species.

Taking into account that pP0 was similar for both conjugates, urea removal of the p64K-βAla[1]pP0 conjugate prior to the immunization experiment could have induced a refolding of the carrier protein in which some βAla[1]pP0 could not be enough exposed in the protein surface and probably impairs an appropriate presentation of the peptide to the immune system of vaccinated animals. In p64K-Cys[1]pP0, the pP0 is linked to Lys residues which are generally exposed on the carrier protein surface. It could be a reason that explains the lower immunogenicity of p64K-βAla[1]pP0 although the N-terminal end and some Lys residues of p64K were also modified with βAla[1]pP0 but in lesser extent to the observed for p64K-Cys[1]pP0. Another explanation for the best immunogenicity of the p64K-Cys[1]pP0 conjugate is that the presence of

Table 1 Efficacy of the p64K-Cys^{1}pP0 and p64K-βAla^{1}pP0 conjugates against *R. sanguineus* infestation in immunized rabbits

Groups	Reduction percent respect to control of			
	Larval yield	Larval viability (%)	Nymph yield	Nymphs' viability (%)
p64k-Cys^{1}pP0 (*n*=4)	57% (73 ± 35)[b]	16% (56 ± 7)[b]	9% (164 ± 62)[a]	24% (74 ± 20)[b]
p64k-βAla^{1}pP0 (*n*=4)	17% (139 ± 57)[a]	13% (67 ± 26)[a]	35% (117 ± 42)[b]	5% (92 ± 5)[a]
PBS (*n*=4, control)	(168 ± 44)[a]	(77 ± 18)[a]	(180 ± 38)[a]	(97 ± 5)[a]
Groups	Reduction percent respect to control of			
	Female yield	Egg mass weight (mg)	Hatchery (%)	*E* (%)
p64k-Cys^{1}pP0 (*n*=4)	0% (21 ± 3)[a]	3% (96.48 ± 32.22)[a]	20% (79 ± 9)[b]	81%
p64k-βAla^{1}pP0 (*n*=4)	0% (21 ± 5)[a]	7% (92.34 ± 31.45)[a]	15% (84 ± 10)[b]	45%
PBS (*n*=4, control)	(20 ± 4)[a]	(99.1 ± 30.12)[a]	(99 ± 2)[a]	

E (efficacy) is calculated as $100 \times [1-(RL \times VL \times RN \times VN \times RA \times PA \times FE)]$ where RL, VL, RN, VN, RA, PA, and FE represent the immunogen effect on larvae yield, larvae viability, nymph yield, nymph viability, female yield, egg mass weight, and egg fertility, respectively. Only parameters showing statistical significant differences compared to those in the control group were included in *E* calculation for each vaccine candidate

In parentheses are shown average ± SD of each recorded parameter

Different letters mean statistically different groups (ANOVA, Bonferroni multiple test, *P* < 0.05)

covalent aggregates with high molecular mass, such as dimmers and multimers observed on SDS-PAGE analysis, turns this conjugate into an antigen more relevant for the immune system of the vaccinated animals [59, 60] because cross-linked aggregates of the carrier protein are absent in the p64K-βAla^{1}pP0 conjugate as shown by the results presented here. In our experience, the pP0 alone or expressed as a fusion protein was not able to induce a strong host immune response (data not shown). The best immunological response and efficacy results obtained with pP0-based vaccines have been obtained after chemical conjugation of this peptide to highly aggregated carrier proteins with very well-ordered quaternary structure and very high molecular masses such as KLH [9–11] and the particulate Bm86 protein expressed intracellularly by *Pichia pastoris* yeast [15, 61]. There are many examples in literature highlighting the role of multimerization and/or aggregation in the generation of an immune response (65, 66), and for the vaccines' development, the immune response enhancement by inducing antigen aggregation in different ways has an important implication. Very recent vaccine reports in the context of COVID-19 pandemic refer also this strategy [62, 63].

The innate immune system has evolved to recognize repetitive patterns present in pathogens and protein aggregates may resemble them [64]. The P64K protein is derived from pathogenic bacteria, *Neisseria meningitidis*, and although recombinant protein expressed in *E. coli* is not a virus-like particle on size exclusion chromatography, it behaves as a dimer/tetramer of 120 or 240 kDa containing several repetitive monomer units of approximately 62kDa each [43]. Probably after chemical conjugation, bmps stabilizes these high molecular mass aggregates as observed in SDS-PAGE analysis of p64K-Cys^{1}pP0 (Fig. 2a). On the other hand, we could hypothesize that the urea usage in the synthesis of p64K-βAla^{1}pP0 conjugate could damage the quaternary structure and the multimerization degree described for intact p64K with the consequent negative impact on its properties as a carrier protein.

All these evidences raise the question whether a controlled covalent aggregation step of p64K should be included in the production process to obtain covalent multimeric conjugates of p64K-Cys^{1}pP0, with enhanced anti-pP0 titers and efficacy.

Conclusions

Rigorous and exhaustive characterization and batch-to-batch consistency of any final product for human use [65] and more recently also for veterinary use under the "one health" concept are requested by regulatory agencies. Homogeneous biomolecules facilitate compliance with this requirement; however, the immunological response and efficacy triggered by the highly heterogeneous p64K-Cys^{1}pP0 conjugate as an anti-tick vaccine candidate were significantly superior to those obtained for a more homogeneous p64K-βAla^{1}pP0 conjugate.

Although both conjugates had a similar pP0/P64K ratio, the high molecular mass aggregates observed in SDS-PAGE analysis of the p64K-Cys^{1}pP0 conjugate could be the responsible to generate a better immune response against pP0 and as

a consequence the best efficacy probably because the peptide presentation to the host immune system was more efficient in this context. The identification by LC-MS/MS analysis of type 2 peptides derived exclusively from the carrier protein with the intact and hydrolyzed linker also supported the presence of these multimers, only observed in p64K-Cys[1]pP0.

Although conjugates are composed just by the chemical linkage between two molecules, their structural complexity demands the usage of different strategies described here to obtain complementary results for their full characterization.

Data availability Raw data and the Electronic Supplemental file (Electronic Supplemental Material_ABC_ p64k-P0.pdf) can be downloaded from http://proteomics.fiocruz.br/ABC_manuscript.

Declarations No violation of animal rights occurred during this investigation. All procedures involving animals followed the Guide for the Care and Use of Laboratory Animals (Council NR. Guide for the care and use of laboratory animals: National Academies Press; 2010) and were approved by the Ethics Committee of the Institutional Animal Care and Use Committee (IACUC #19088).

Ethics approval Consent to submit this manuscript has been received from all co-authors.

Conflict of interest The authors declare no competing interests.

References

1. Nicholson WL, Sonenshine DE, Noden BH, Brown RN. Ticks (Ixodida). In: Medical and veterinary entomology: Elsevier; 2019. p. 603–72.
2. Rodriguez-Vivas R, Trees A, Rosado-Aguilar J, Villegas-Perez S, Hodgkinson J. Evolution of acaricide resistance: phenotypic and genotypic changes in field populations of Rhipicephalus (Boophilus) microplus in response to pyrethroid selection pressure. Int J Parasitol. 2011;41(8):895–903.
3. Valle MR, Mendez L, Valdez M, Redondo M, Espinosa CM, Vargas M, et al. Integrated control of Boophilus microplus ticks in Cuba based on vaccination with the anti-tick vaccine Gavac. Exp Appl Acarol. 2004;34(3-4):375–82.
4. Suarez M, Rubi J, Pérez D, Cordova V, Salazar Y, Vielma A, et al. High impact and effectiveness of Gavac™ vaccine in the national program for control of bovine ticks Rhipicephalus microplus in Venezuela. Livest Sci. 2016;187:48–52.
5. Schetters T, Bishop R, Crampton M, Kopacek P, Lew-Tabor A, Maritz-Olivier C, et al. Cattle tick vaccine researchers join forces in CATVAC. Parasit Vectors. 2016;9:105.
6. de la Fuente J, Rodriguez M, Montero C, Redondo M, Garcia-Garcia JC, Mendez L, et al. Vaccination against ticks (Boophilus spp.): the experience with the Bm86-based vaccine Gavac. Genet Anal: Biomol Eng. 1999;15(3-5):143–8.
7. Jonsson N, Matschoss A, Pepper P, Green P, Albrecht M, Hungerford J, et al. Evaluation of TickGARDPLUS, a novel vaccine against Boophilus microplus, in lactating Holstein–Friesian cows. Vet Parasitol. 2000;88(3-4):275–85.
8. De La Fuente J, Rodríguez M, Redondo M, Montero C, García-García J, Méndez L, et al. Field studies and cost-effectiveness analysis of vaccination with Gavac™ against the cattle tick Boophilus microplus. Vaccine. 1998;16(4):366–73.
9. Rodriguez-Mallon A, Encinosa PE, Mendez-Perez L, Bello Y, Rodriguez Fernandez R, Garay H, et al. High efficacy of a 20 amino acid peptide of the acidic ribosomal protein P0 against the cattle tick, Rhipicephalus microplus. Ticks Tick Borne Dis. 2015;6(4):530–7.
10. Rodriguez-Mallon A, Fernandez E, Encinosa PE, Bello Y, Mendez-Perez L, Ruiz LC, et al. A novel tick antigen shows high vaccine efficacy against the dog tick, Rhipicephalus sanguineus. Vaccine. 2012;30(10):1782–9.
11. Rodríguez-Mallon A, Encinosa Guzmán PE, Bello Soto Y, Rosales Perdomo K, Montero Espinosa C, Vargas M, et al. A chemical conjugate of the tick P0 peptide is efficacious against Amblyomma mixtum. Transbound Emerg Dis. 2020;67:175–7.
12. Harris JR, Markl J. Keyhole limpet hemocyanin: molecular structure of a potent marine immunoactivator. A review. Eur Urol. 2000;37(Suppl 3):24–33.
13. Swerdlow RD, Ebert RF, Lee P, Bonaventura C, Miller KI. Keyhole limpet hemocyanin: structural and functional characterization of two different subunits and multimers. Comp Biochem Physiol B: Biochem Mol Biol. 1996;113(3):537–48.
14. Heldens J, Patel J, Chanter N, Ten Thij G, Gravendijck M, Schijns V, et al. Veterinary vaccine development from an industrial perspective. Vet J. 2008;178(1):7–20.
15. Rodriguez Mallon A, Javier Gonzalez L, Encinosa Guzman PE, Bechara GH, Sanches GS, Pousa S, et al. Functional and mass spectrometric evaluation of an anti-tick antigen based on the P0 peptide conjugated to Bm86 protein. Pathogens. 2020;9(6):513–37.
16. Guillen G, Alvarez A, Silva R, Morera V, Gonzalez S, Musacchio A, et al. Expression in Escherichia coli of the lpdA gene, protein sequence analysis and immunological characterization of the P64k protein from Neisseria meningitidis. Biotechnol Appl Biochem. 1998;27(3):189–96.
17. Gonzalez S, Alvarez A, Caballero E, Vina L, Guillen G, Silva R. P64k meningococcal protein as immunological carrier for weak immunogens. Scand J Immunol. 2000;52(2):113–6.
18. Carmenate T, Canaan L, Alvarez A, Delgado M, Gonzalez S, Menendez T, et al. Effect of conjugation methodology on the immunogenicity and protective efficacy of meningococcal group C polysaccharide-P64k protein conjugates. FEMS Immunol Med Microbiol. 2004;40(3):193–9.
19. Guirola M, Urquiza D, Alvarez A, Cannan-Haden L, Caballero E, Guillen G. Immunologic memory response induced by a meningococcal serogroup C conjugate vaccine using the P64k recombinant protein as carrier. FEMS Immunol Med Microbiol. 2006;46(2):169–79.
20. Perez AE, Dickinson FO, Banderas F, Serrano T, Llanes R, Guzman D, et al. Safety and preliminary immunogenicity of MenC/P64k, a meningococcal serogroup C conjugate vaccine with a new recombinant carrier. FEMS Immunol Med Microbiol. 2006;46(3):386–92.

21. Hermida L, Rodriguez R, Lazo L, Bernardo L, Silva R, Zulueta A, et al. A fragment of the envelope protein from dengue-1 virus, fused in two different sites of the meningococcal P64k protein carrier, induces a functional immune response in mice. Biotechnol Appl Biochem. 2004;39(Pt 1):107–14.

22. Izquierdo A, Garcia A, Lazo L, Gil L, Marcos E, Alvarez M, et al. A tetravalent dengue vaccine containing a mix of domain III-P64k and domain III-capsid proteins induces a protective response in mice. Arch Virol. 2014;159(10):2597–604.

23. Valdes I, Hermida L, Martin J, Menendez T, Gil L, Lazo L, et al. Immunological evaluation in nonhuman primates of formulations based on the chimeric protein P64k-domain III of dengue 2 and two components of Neisseria meningitidis. Vaccine. 2009;27(7):995–1001.

24. Fields GB, Noble RL. Solid phase peptide synthesis utilizing 9-fluorenylmethoxycarbonyl amino acids. Int J Pept Protein Res. 1990;35(3):161–214.

25. Laemmli UK. Cleavage of structural proteins during the assembly of the head of bacteriophage T4. Nature. 1970;227(5259):680–5.

26. Rivera B, Leyva A, Portela MM, Moratorio G, Moreno P, Durán R, et al. Quantitative proteomic dataset from oro-and naso-pharyngeal swabs used for COVID-19 diagnosis: detection of viral proteins and host's biological processes altered by the infection. Data Brief. 2020;32:106121.

27. Chen ZL, Meng JM, Cao Y, Yin JL, Fang RQ, Fan SB, et al. A high-speed search engine pLink 2 with systematic evaluation for proteome-scale identification of cross-linked peptides. Nat Commun. 2019;10(1):3404.

28. Hoopmann MR, Zelter A, Johnson RS, Riffle M, MacCoss MJ, Davis TN, et al. Kojak: efficient analysis of chemically cross-linked protein complexes. J Proteome Res. 2015;14(5):2190–8.

29. Gotze M, Pettelkau J, Schaks S, Bosse K, Ihling CH, Krauth F, et al. StavroX–a software for analyzing crosslinked products in protein interaction studies. J Am Soc Mass Spectrom. 2012;23(1):76–87.

30. Yılmaz Ş, Shiferaw GA, Rayo J, Economou A, Martens L, Vandermarliere E. Cross-linked peptide identification: a computational forest of algorithms. Mass Spectrom Rev. 2018;37(6):738–49.

31. Schilling B, Row RH, Gibson BW, Guo X, Young MM. MS2Assign, automated assignment and nomenclature of tandem mass spectra of chemically crosslinked peptides. J Am Soc Mass Spectrom. 2003;14(8):834–50.

32. Kall L, Canterbury JD, Weston J, Noble WS, MacCoss MJ. Semi-supervised learning for peptide identification from shotgun proteomics datasets. Nat Methods. 2007;4(11):923–5.

33. Boyatzis AE, Bringans SD, Piggott MJ, Duong MN, Lipscombe RJ, Arthur PG. Limiting the Hydrolysis and Oxidation of Maleimide-Peptide Adducts Improves Detection of Protein Thiol Oxidation. J Proteome Res. 2017;16(5):2004–15.

34. Ma B, Zhang K, Hendrie C, Liang C, Li M, Doherty-Kirby A, et al. PEAKS: powerful software for peptide de novo sequencing by tandem mass spectrometry. Rapid Commun Mass Spectrom : RCM. 2003;17(20):2337–42.

35. Council NR. Guide for the care and use of laboratory animals: National Academies Press; 2010.

36. Leroux-Roels G. Unmet needs in modern vaccinology: adjuvants to improve the immune response. Vaccine. 2010;28:C25–36.

37. Heegaard PM, Dedieu L, Johnson N, Le Potier M-F, Mockey M, Mutinelli F, et al. Adjuvants and delivery systems in veterinary vaccinology: current state and future developments. Arch Virol. 2011;156(2):183–202.

38. Encinosa Guzmán PE, Bello Soto Y, Rodríguez-Mallon A. Genetic and biological characterization of a Cuban tick strain from Rhipicephalus sanguineus complex and its sensitivity to different chemical acaricides. Int J Acarol. 2016;42(1):18–25.

39. Rodríguez-Mallon A. Developing anti-tick vaccines. Vaccine Design: Springer; 2016. p. 243–59.

40. Perez-Perez D, Bechara GH, Machado R, Andrade G, Del Vecchio R, Pedroso M, et al. Efficacy of the Bm86 antigen against immature instars and adults of the dog tick Rhipicephalus sanguineus (Latreille, 1806)(Acari: Ixodidae). Vet Parasitol. 2010;167(2-4):321–6.

41. Schnupf P, Sansonetti PJ. Quantitative RT-PCR profiling of the rabbit immune response: assessment of acute Shigella flexneri infection. PLoS One. 2012;7(6):e36446.

42. Shi Y, Mowery RA, Ashley J, Hentz M, Ramirez AJ, Bilgicer B, et al. Abnormal SDS-PAGE migration of cytosolic proteins can identify domains and mechanisms that control surfactant binding. Protein Sci. 2012;21(8):1197–209.

43. Gómez R, Madrazo J, González L, Chinea G, Musacchio A, Rodríguez A, et al. Caracterización estructural y funcional de la proteína recombinante P64k de Neisseria meningitidis. Biotecnol Apl. 1999;16(2):83–7.

44. Bringas R, Fernandez J. A lipoamide dehydrogenase from Neisseria meningitidis has a lipoyl domain. Proteins: Struct., Funct., Genet. 1995;21(4):303–6.

45. Wakankar AA, Feeney MB, Rivera J, Chen Y, Kim M, Sharma VK, et al. Physicochemical stability of the antibody− drug conjugate trastuzumab-DM1: changes due to modification and conjugation processes. Bioconjug Chem. 2010;21(9):1588–95.

46. van Vught R, Pieters RJ, Breukink E. Site-specific functionalization of proteins and their applications to therapeutic antibodies. Comput Struct Biotechnol J. 2014;9:e201402001.

47. Li de la Sierra I, Pernot L, Prange T, Saludjian P, Schiltz M, Fourme R, et al. Molecular structure of the lipoamide dehydrogenase domain of a surface antigen from Neisseria meningitidis. J Mol Biol. 1997;269(1):129–41.

48. de la Sierra IL, Prangé T, Fourme R, Padrón G, Fuentes P, Musacchio A, et al. Crystallization and preliminary X-ray investigation of a recombinant outer membrane protein from Neisseria meningitidis. J Mol Biol. 1994;235(3):1154–5.

49. Kratz H, Haeckel A, Michel R, Schönzart L, Hanisch U, Hamm B, et al. Straightforward thiol-mediated protein labelling with DTPA: synthesis of a highly active 111 In-annexin A5-DTPA tracer. EJNMMI Res. 2012;2(1):1–7.

50. Brewer CF, Riehm JP. Evidence for possible nonspecific reactions between N-ethylmaleimide and proteins. Anal Biochem. 1967;18(2):248–55.

51. Trnka MJ, Baker PR, Robinson PJ, Burlingame AL, Chalkley RJ. Matching cross-linked peptide spectra: only as good as the worse identification. Mol Cell Proteomics : MCP. 2014;13(2):420–34.

52. Yu F, Li N, Yu W. Exhaustively identifying cross-linked peptides with a linear computational complexity. J Proteome Res. 2017;16(10):3942–52.

53. Harrison AG, Young AB. Fragmentation reactions of deprotonated peptides containing proline. The proline effect. J Mass Spectrom : JMS. 2005;40(9):1173–86.

54. Chen JJ, Lin WJ, Shieh PC, Chen IS, Peng CF, Sung PJ. A new long-chain alkene and antituberculosis constituents from the leaves of Pourthiaea lucida. Chem Biodivers. 2010;7(3):717–21.

55. Giese SH, Fischer L, Rappsilber J. A study into the collision-induced dissociation (CID) behavior of cross-linked peptides. Mol Cell Proteomics. 2016;15(3):1094–104.

56. Chavez JD, Eng JK, Schweppe DK, Cilia M, Rivera K, Zhong X, et al. A general method for targeted quantitative cross-linking mass spectrometry. PLoS One. 2016;11(12):e0167547.

57. Müller-Doblies U, Maxwell S, Boppana V, Mihalyo M, Mcsorley SJ, Vella A, et al. Feeding by the tick, Ixodes scapularis, causes CD4+ T cells responding to cognate antigen to develop the capacity to express IL-4. Parasite Immunol. 2007;29(10):485–99.

58. Tabor AE, Ali A, Rehman G, Rocha Garcia G, Zangirolamo AF, Malardo T, et al. Cattle tick Rhipicephalus microplus-host interface: a review of resistant and susceptible host responses. Front Cell Infect Microbiol. 2017;7:506.

59. Wang W, Singh SK, Li N, Toler MR, King KR, Nema S. Immunogenicity of protein aggregates—concerns and realities. Int J Pharm. 2012;431(1-2):1–11.

60. Hermeling S, Crommelin DJ, Schellekens H, Jiskoot W. Structure-immunogenicity relationships of therapeutic proteins. Pharm Res. 2004;21(6):897–903.

61. García-García J, Montero C, Rodriguez M, Soto A, Redondo M, Valdés M, et al. Effect of particulation on the immunogenic and protective properties of the recombinant Bm86 antigen expressed in Pichia pastoris. Vaccine. 1998;16(4):374–80.

62. Dai L, Zheng T, Xu K, Han Y, Xu L, Huang E, et al. A universal design of betacoronavirus vaccines against COVID-19, MERS, and SARS. Cell. 2020;182(3):722–33. e11.

63. Walls AC, Fiala B, Schäfer A, Wrenn S, Pham MN, Murphy M, et al. Elicitation of potent neutralizing antibody responses by designed protein nanoparticle vaccines for SARS-CoV-2. Cell. 2020;183(5):1367–82. e17.

64. Rosenberg AS. Effects of protein aggregates: an immunologic perspective. AAPS J. 2006;8(3):E501–E7.

65. International Conference on Harmonisation; guidance on specifications: test procedures and acceptance criteria for biotechnological/biological products. Notice. Food and Drug Administration, HHS. Fed Regist. 1999;64(159):44928–35.

Publisher's note Springer Nature remains neutral with regard to jurisdictional claims in published maps and institutional affiliations.